

# Improved Vessel Segmentation Using Curvelet Transform and Line Operators

Renoh Johnson Chalakkal and Waleed H. Abdulla  
The University of Auckland, New Zealand  
E-mail: renoh.chalakkal,w.abdulla@auckland.ac.nz

**Abstract**—Vessel segmentation from the fundus retinal images is highly significant in diagnosing many pathologies related to eye and other systemic diseases. Even though there are many methods in the literature focusing on this task, most of these methods are not focusing on the small peripheral vessels segmentation. In this paper, we propose a new approach based on curvelet transform and line operators which can segment the small peripheral vessels with very high accuracy resulting in a higher sensitivity compared to the other state-of-the-art methods. In the proposed approach, the contrast between the retinal vessels and the background pixels is enhanced by applying a series of image processing steps involving color space transformation, adaptive histogram equalization, and anisotropic diffusion filtering. Then by using the modified curvelet transform coefficients, the retinal vessel edge contrast is further enhanced. Finally, the vessels are segmented out by applying the line operator response, followed by suitable thresholding to obtain the segmented vessels. Post processing is carried out to remove the scattered unwanted background pixels. The performance of the method is compared against the other state-of-the-art methods using DRIVE as a testing database. An average sensitivity, specificity, accuracy and positive predictive value of 0.7653, 0.9735, 0.9542 and 0.7438 are respectively achieved.

## I. INTRODUCTION

Vessels segmentation from retinal images has remained a challenging research topic for the last few years. The information that is obtained from the segmented vessels like vessel width, vessel tortuosity, new vessels formation on the optic disc and elsewhere, etc. are of great significance in the field of automatic retinal image analysis. One of the main application of the vessel segmentation is in the development of automated systems that could detect the presence of various pathologies like hypertension, glaucoma, diabetic retinopathy (DR), macular edema etc., using the retinal fundus image. The retinal vessels undergo significant changes in its standard structure when the particular subject is under the influence of any such pathologies. A very prominent change in the vessel structure in the form of variation in the vessel tortuosity and presence of new vessels are visible in the retinal image affected by severe DR. Also retinal vessels could be used as a reference for detecting other vital structures like optic disc and fovea in the retinal image.

Automatic vessel segmentation methods can be classified into two categories: supervised and unsupervised. The supervised techniques need labeled images for the training phase, wherein a system (machine learning based or deep learning based) is first trained on many training images. Once the

system is trained, the performance of the system is evaluated on a different (mutually exclusive) testing set. Recently there have been a few supervised methods based on deep learning [1], [2], [3] that have achieved better segmentation performance compared to other methods (both supervised and unsupervised). The significant disadvantages of deep learning based methods are the computational complexity and resources required for the training and testing phase. Also since the number of manually segmented versions of the vessels (taken as ground truths) is limited (20 in STARE database [4] and 40 in DRIVE database [5]), the images used in training phase are limited. Various augmentation methods are then used to increase the number of samples in the training sets. This limitation results in better performance of the technique on one database (from which the images are included in the training set), but a reduced performance on another database (for images not included in the training set).

In this paper, we propose a new unsupervised vessel segmentation technique, which can segment the small/tiny vessels along with the other main vessels. Since the method is unsupervised, the database size restrictions are negotiated. This method is an improved version of our previous method discussed in [6]. The main advantage of the current method over our previous method is a higher sensitivity (*SE*) and positive predictive value (*PPV*). The proposed method can segment more vessel pixels belonging to the small/tiny vessels.

This paper is organized as follows. Section II discusses a few recent supervised and unsupervised techniques that are focused on the same task of vessel segmentation. In section III, the proposed algorithm is detailed. Section IV reports the performance and comparison of the proposed method with other state-of-the-art methods including our previous method [6]. Section V concludes this paper and portrays the future direction of this work.

## II. RECENT ADVANCEMENTS IN VESSEL SEGMENTATION

Recently, there have been significant research interests in the field of automatic retinal image analysis, specifically the retinal vessel segmentation. With the advancement of the deep learning techniques, this research problem has become more interesting. The retinal vessel segmentation approaches can be grouped into two broad categories: supervised and unsupervised. The supervised method relies on the quality and correctness of the ground truth images that are acting as the reference standard for these methods. In [1], a

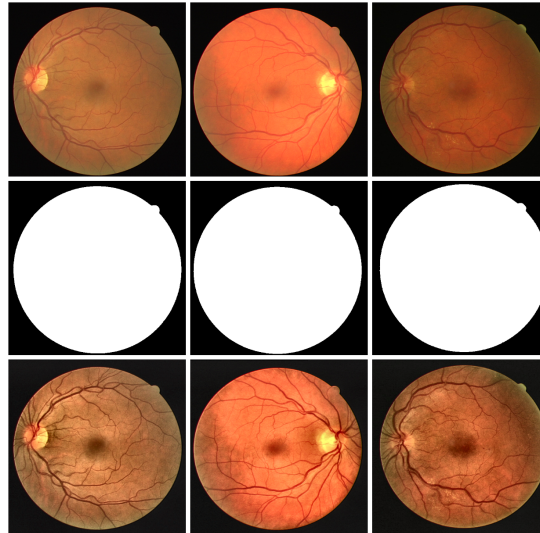


Fig. 1. Preprocessing: First row shows the input retinal images ('01\_test.tif', '02\_test.tif' and '03\_test.tif') from DRIVE database, the second row shows the respective masks generated and the third row presents the final pre-processed image (' $I_p$ ')

deep learning based vessel segmentation is discussed. They have used convolutional neural networks (CNNs) and fully-connected conditional random fields (CRFs) to obtain a vessel probability map, which is then thresholded to get the binary vessel segmentation result. They have reported an accuracy ( $Acc$ ) of 0.9470 with a sensitivity ( $SE$ ) of 0.7294 on DRIVE database. They have reported in the paper that their method is affected by the cross-learning problem, which is due to the limitation of the number of training images. This can be a significant disadvantage with the supervised techniques employed in the field of retinal image processing.

In [2], another deep learning based method is discussed. They used a pixel level classification by classifying the pixels in each image. The reported  $Acc$  and  $SE$  are 0.9466 and 0.7276 respectively. The main disadvantage of this method is the time and the resources (memory, graphics processing unit (GPU), etc.) needed for the training and testing phases. Also since it is a pixel level classification, it is also susceptible to the pathological regions inside the retinal images, and thus the misclassification probability is high. Other supervised methods are discussed in [3], [7], [8], [9], [10]. The performance metrics of these methods are reflected in Table II.

Among the unsupervised methods, our previous method detailed in [6] was able to achieve a segmentation  $Acc$  of 0.9518. But, this method was not able to segment small/tiny vessels effectively. Hence the  $SE$  and positive prediction value ( $PPV$ ) for this method was 0.7386 and 0.7162 respectively. Our main motive to develop the proposed method is to detect and segment the small/tiny vessels more accurately which results in better  $SE$  and  $PPV$ . Other unsupervised methods are discussed in [11], [12], [13], [14], [15] and their performance metrics are also reflected in Table II in section IV.

In this paper, we have discussed a new unsupervised method for the vessel segmentation, which is computationally less complicated and easy to implement. The performance of the proposed method is superior to other supervised and unsupervised state-of-the-art methods as shown in Table II in section IV.

### III. THE PROPOSED METHOD

In [6], we have discussed a vessel segmentation method that was based on contrast enhancement of the retinal vessel edges and then using a fuzzy C-mean to segment/extract the vessels. The main disadvantage of this method was that it failed to segment small/tiny vessel pixels and hence resulted in a lower  $PPV$  value. In the proposed method we worked on improving the sensitivity and the  $PPV$  by using a new version of vessel edge enhancement algorithm based on fast discrete curvelet transform (FDCT). Also, we have used a modified line detector method using variable length with a resolution of  $10^\circ$  for segmenting/extracting vessel pixels instead of the fuzzy C-mean classification used in [6], which skipped small/tiny vessel pixels. The proposed approach can be abstracted by the following steps:

#### A. Pre-processing stage

The method starts with a pre-processing of the input retinal image ( $I_{in}$ ) stage. The input  $RGB$  image is first resized to  $500 \times 500 \times 3$  from the original resolution of  $565 \times 584 \times 3$ . The resized image is then converted to the  $CIEL^*a^*b$  color space [16], [17] to extract the lightness information (' $L$ ') from it.  $CIEL^*a^*b$  color space consists of three components, the ' $L$ ' component carrying the lightness information and the ' $a$ ' and ' $b$ ' components carrying the chromaticity or color information. Adaptive histogram equalization [18] is



Fig. 2. Vessel edge enhancement: a) Pre-processed image ( $I_p$ ) b) first vessel enhanced sub-image ( $I_1$ ) c) second vessel enhanced sub-image ( $I_2$ )

then applied to this  $CIEL * a * b$  converted image. Noise is introduced as a consequence of this step. So anisotropic diffusion filtering [19] is applied on the histogram equalized image. The image obtained after the filtering is converted back to  $RGB$  color space. Weighted scaling [20] is carried out to convert the  $RGB$  converted image into a gray-scale image ( $I_{gray}$ ) for further processing.

A retinal mask is generated to extract the field of view (FOV). The mask generation is based on morphological operations like opening, closing, erosion, and dilation [21]. In most retinal images, the red channel has very high pixel intensities within the fundus region and low pixel intensities outside the fundus region. Hence after applying the edge detection based on Laplacian of Gaussian method [22], these morphological operations are carried out on the red channel of the original image ( $I_{in}$ ). The mask generated ( $I_{mask}$ ) for few images from the DRIVE [5] database are shown in Fig.1. The mask is then applied on to the gray-scale converted image ( $I_{gray}$ ) to obtain the pre-processed image ( $I_p$ ).

### B. Vessel edge enhancement

In order to improve the vessel edge strength, a modified version of the method discussed in [6], based on fast discrete curvelet transform (FDCT) [23] is applied on the pre-processed image ( $I_p$ ). FDCT has been used by few other state-of-the art methods [24], [25], [26], to enhance the retinal image contrast. FDCT is a multiscale transform that could be used to handle the singularities present in a retinal image and could selectively enhance the vessel edge contrast compared to the background pixels.  $I_p$  in the spatial domain can be represented as  $I_p(t_1, t_2)$ , where  $0 \leq t_1, t_2 \leq n$ . 2-D FFT is applied on  $I_p$  to obtain the Fourier samples,  $\hat{I}_p[n_1, n_2]$ , where  $-\frac{n}{2} \leq n_1, n_2 \leq \frac{n}{2}$ . Multiply the Fourier samples  $\hat{I}_p[n_1, n_2]$  with the discrete localising window  $\tilde{J}_{j,l}[n_1, n_2]$  (used for digital coronization in wrapping based FDCT), where ‘ $j$ ’ is the scale and ‘ $l$ ’ is the angle and wrap the product around the origin to obtain  $\tilde{I}_{p,j,l}[n_1, n_2]$  given by Eq.1.

$$\tilde{I}_{p,j,l}[n_1, n_2] = W(\tilde{J}_{j,l}\hat{I}_p)[n_1, n_2] \quad (1)$$

where the range for  $n_1$  and  $n_2$  is now  $0 \leq n_1 \leq Z_{1,j}$  and  $n_2 < Z_{2,j}$ .  $Z_{1,j} \sim 2^j$  and  $Z_{2,j} \sim 2^{j/2}$  are constants. Finally inverse 2-D FFT is applied to each  $\tilde{I}_{p,j,l}$  to obtain the discrete curvelet

TABLE I  
PARAMETER VALUES FOR THE MODIFYING FUNCTION

Parameter	Range	Used value
$w_1$	$w_1 \geq 1$	1.5
$w_2$	$w_2 \geq 1$	2
$w_3$	$w_3 > 0$	2
$a$	$0 < a < \frac{m}{\sigma}$	1.5
$p$	$0 < p < 1$	0.5

coefficients  $c^D(j, l, k)$ , where  $k = (k_1, k_2)$  is the translation parameter.

The FDCT coefficients obtained are then selectively amplified/suppressed, depending on the level of approximation (coarse and fine) needed, that could enhance the vessel edge contrast. There is a trade-off in selecting a particular modifying function to amplify the FDCT coefficients of the fine approximation by suppressing the coarse approximation of the pre-processed image,  $I_p$ . Hence compared to the modifying function selected in [6], in this method we developed a modifying function that can simultaneously amplify the fine approximations and suppress the coarse coefficients of the FDCT coefficients. Instead of a crisp decision in suppressing the coarse coefficients to zero (which could actually leave some vessel pixels residue), the coefficients are soft masked to a low value compared to the other FDCT coefficients. The modifying function ‘ $\kappa$ ’ selected is given in Eq.2.

$$\kappa(c) = \begin{cases} w_1 \cdot \left(\frac{m}{\sigma}\right)^p, & \text{if } |c| < a\sigma. \\ w_2 \cdot \left(\frac{m}{|c|}\right)^p, & \text{if } a\sigma \leq |c| < m. \\ w_3, & \text{if } |c| \geq m. \end{cases} \quad (2)$$

where ‘ $c$ ’ is the input FDCT coefficient, ‘ $\sigma$ ’ is the noise standard deviation of the curvelet coefficients of the relative band which are in the same direction and scale, calculated using the method specified in [27]. ‘ $m$ ’ is the maximum FDCT coefficient of the respective band for which the modifying parameter is calculated.  $w_1, w_2, w_3, a$  and  $p$  used in Eq.2 are given in Table I. These values are selected heuristically, which resulted in a better segmentation performance (including the small/tiny vessels). After applying the modifying function, the vessel edge weight image ( $I_{w1}$ ) is obtained by taking the inverse discrete curvelet transform (IDCT).

Parallel to the above steps, a series of other image processing steps are carried out on the pre-processed retinal image ( $I_p$ ), which are explained in Eq.3 to Eq.6.  $I_p$  is low-pass filtered using a median filter of size  $20 \times 20$ , which is then subtracted from the green channel of the input image  $I_{in}$ , to obtain another weight image  $I_{w2}$ . This image is then thresholded to detect the pixels with negative intensity values, which is then morphologically processed to obtain the optic disc removed and vessel edge enhanced image ( $I_1$ ) as shown in Fig.2.(b). This image is then subtracted from the vessel edge weight image ( $I_{w1}$ ), and the output is complemented to obtain the second vessel edge enhanced image ( $I_2$ ) as shown in Fig. 2.(c).

$$I_{filtered} = LPF(I_p) \quad (3)$$

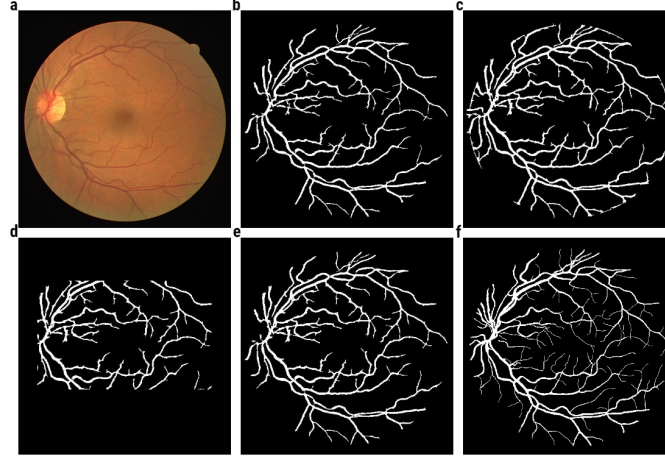


Fig. 3. Vessel edge enhancement: a) Input image ('01\_test.tif') from DRIVE database b) segmented vessels from 'I<sub>1</sub>' ('I<sub>Out1</sub>') c) segmented vessels from 'I<sub>2</sub>' ('I<sub>Out2</sub>') d) image obtained after applying mask e) final version of the segmented vessel image ('I<sub>vessel</sub>') f) ground truth image ('01\_manual1.gif')

$$I_{w2} = I_{in,green} - I_{filtered} \tag{4}$$

$$I_1 = (I_{w2} \leq 0) \tag{5}$$

$$I_2 = (I_{w1} - I_1)^C \tag{6}$$

where 'C' in Eq. 6 represents the compliment taken.

These two images (I<sub>1</sub> and I<sub>2</sub>) are used in the next step, where we applied a modified line detection technique to detect the retinal vessels.

### C. Vessel segmentation

We have used a modified version of line detector with a variable length ranging from  $l_{LD} = 1$  to  $l_{LD} = 21$  pixels, with 18 angles having a resolution of 10° each. The idea behind this method is derived from a technique discussed in [8]. We have increased the number of angles (to 18) and also the possible length of the line (to 21 pixels) in this method. This resulted in a better segmentation performance (*SE* and *PPV*), which could also segment the small and tiny vessel pixels from the vessel edge enhanced images I<sub>1</sub> and I<sub>2</sub>.

The line detector is applied on both I<sub>1</sub> and I<sub>2</sub> images simultaneously by taking a sliding window of dimension (21 × 21). When a pixel (i, j) falls within a vessel, the line detector passing through that pixel will have a higher gray level. The gray level for each pixel in the respective window is evaluated for 18 different orientations using lines of fixed length 'l<sub>LD</sub>'. The gray level for each pixel within 'l<sub>LD</sub>' is also calculated. It is found that the segmentation performance was the best when l<sub>LD</sub> = 17 pixels.

After obtaining the largest average gray level (L<sub>gray</sub>(i, j)) for each pixel in a particular window, it is subtracted from the average gray level (M<sub>gray</sub>(i, j)) of the entire pixels in that respective window centered at (i, j) to obtain the line strength S(i, j) for each pixel (i, j) in the images I<sub>1</sub> and I<sub>2</sub>. S(i, j)

will be higher when a line completely lies inside a vessel and will be lower for pixels lying outside the vessels.

The S(i, j) image is then thresholded using 2D Otsu thresholding technique discussed in [28]. The thresholded images (I<sub>Out1</sub> and I<sub>Out2</sub>) after this step are shown in Fig.3(b-c). Fig.3.(c) shows that I<sub>Out2</sub> contains more small/tiny vessel pixels in the central region of the FOV. But it also has more false positive pixels (pixels detected as vessels that are not vessels) near the outer boundary of the FOV. Hence we created a binary mask having dimensions 250 × 250 centered at the pixel (i, j) = (250, 250). The image obtained after applying this mask on the I<sub>Out2</sub> is added to the I<sub>Out1</sub> to obtain the final version of the segmented vessel image I<sub>vessel</sub> shown in Fig.3.(e). Fig.3.(f) shows the ground truth image available in the DRIVE database, which is manually segmented. Then by applying morphological operations (like opening, closing, erosion, and dilation) and connected component analysis [29], the non-vessel pixels are removed.

From Fig.3.(e-f), it can be seen that the proposed method can detect small/tiny vessels as accurately as in the manually segmented version. Even though there are few very small vessels missed, the information about these vessel pixels is not as significant as the other major and small vessels in the automatic retinal image analysis.

## IV. RESULTS AND DISCUSSION

The proposed method is tested on DRIVE database [5] images. DRIVE database was selected because it is widely used by the researchers to report the performance of their retinal vessel segmentation algorithms. Thus algorithms can be compared. The performance of the proposed approach is reported in terms of sensitivity (*SE*), specificity (*SP*), positive predictive value (*PPV*) and accuracy (*Acc*). These metrics are defined as follow:

$$SE = \frac{TP}{TP + FN} \tag{7}$$

$$SP = \frac{TN}{TN + FP} \quad (8)$$

$$PPV = \frac{TP}{TP + FP} \quad (9)$$

$$Acc = \frac{TP + TN}{TP + TN + FP + FN} \quad (10)$$

where,

- $TP$  = True positive (pixels segmented out from the retinal image as vessel which are actually vessels in the ground truth image)
- $TN$  = True Negative (pixels segmented out from the retinal image as non-vessel which are actually non-vessels in the ground truth image)
- $FP$  = False Positive (pixels segmented out from the retinal image as vessel which are actually non-vessels in the ground truth image)
- $FN$  = False Negative (pixels segmented out from the retinal image as non-vessel which are actually vessels in the ground truth image)

The performance of the proposed approach is reported in Table. II based on the above metrics. It can be seen from the Table. II that the proposed method has the best  $SE$  among the other state-of-the-art methods. The  $SE$  of the proposed method has been improved over our previous method discussed in [6]. The main reason for this is that the proposed method can segment increased number of small/tiny vessel pixels along with the other major vessel pixels. The method also has a  $SP$  of over 97%. Compared to other unsupervised methods, the proposed method reports the highest average  $Acc$  of 95.42%. Even though the average  $Acc$  of the technique discussed in [8] is higher, the  $SE$  reported is less compared to the proposed method. It reflects a better vessel segmentation performance to detect more small/tiny vessels pixels.

Fig. 4 shows a comparison between the proposed method and our previous method discussed in [6] in segmenting out the small/tiny vessels from the retinal image. It can be seen that the proposed method is able to segment more small/tiny vessel pixels. Hence the proposed method has a higher  $SE$  compared to the previous method, without compromising on the  $SP$ . This is evident from the fact that the proposed method has a higher overall  $PPV$  of 0.7438 compared to 0.7162 for the method discussed in [6].

Most of the state-of-the-art methods have not mentioned the  $PPV$  achieved and hence we have not mentioned the  $PPV$  achieved using the proposed method in the Table. II. The overall  $Acc$ ,  $SE$ ,  $SP$ , and  $PPV$  of the proposed method over the entire 40 images (including the images in the test and training set of DRIVE database) in the DRIVE database is 0.9538, 0.7249, 0.977, and 0.7582 respectively.

### V. CONCLUSIONS

This paper presents a novel method to segment retinal vessels accurately. A vessel edge enhancement technique using curvelet transform and color space transformation together

TABLE II  
PERFORMANCE COMPARISON WITH STATE-OF-THE-ART METHODS

Method	Year	Class	$SE$	$SP$	$Acc$
Huazhu <i>et al.</i> [1]	2016	Supervised	0.7294	-	0.9470
Melinscak <i>et al.</i> [2]	2015	Supervised	0.7276	0.9785	0.9466
Maji <i>et al.</i> [3]	2015	Supervised	0.6287	-	0.9327
Vega <i>et al.</i> [7]	2015	Supervised	0.7444	0.9600	0.9412
Sohini <i>et al.</i> [10]	2015	Supervised	0.7249	0.9830	0.9519
Fraz <i>et al.</i> [9]	2012	Supervised	0.7406	0.9807	0.9480
Ricci <i>et al.</i> [8]	2007	Supervised	0.7000	0.9600	0.9595
<b>Proposed</b>	<b>2018</b>	<b>Unsupervised</b>	<b>0.7653</b>	<b>0.9735</b>	<b>0.9542</b>
Chalakkal <i>et al.</i> [6]	2017	Unsupervised	0.7386	0.9769	0.9518
Zhao <i>et al.</i> [11]	2014	Unsupervised	0.7354	0.9789	0.9477
Fraz <i>et al.</i> [12]	2012	Unsupervised	0.7152	0.9759	0.9430
Al-Diri <i>et al.</i> [15]	2009	Unsupervised	0.7282	0.9551	-
Mendonica <i>et al.</i> [14]	2006	Unsupervised	0.7344	0.9764	0.9452
Jiang <i>et al.</i> [13]	2003	Unsupervised	-	-	0.9212

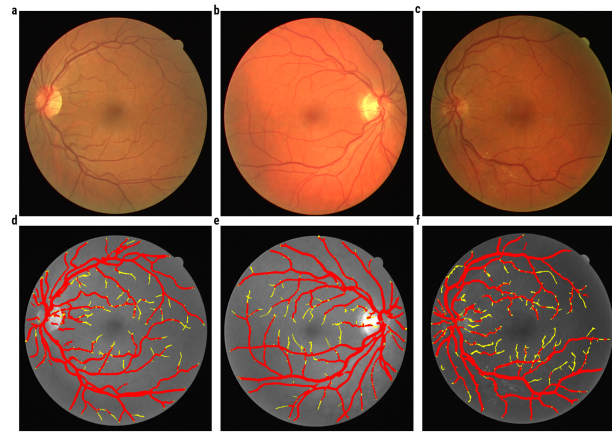


Fig. 4. Comparison between the proposed approach and our previous method [6]: a, b and c represents images from the DRIVE database, and d, e, and f show the segmented vessel pixels respectively. The yellow colored pixels represent the small/tiny vessels that were segmented by the proposed method, in addition to the other vessel pixels (red) that were segmented by our previous method.

with adaptive histogram equalization and anisotropic diffusion filtering is applied to pre-process and enhance the vessel edge contrast. Then by using a line operator, the segmentation of vessel pixel is performed. The results show that the proposed method is able to segment the small/tiny retinal vessels with improved  $Acc$  and  $SE$  compared to other state-of-the-art supervised and unsupervised methods. The technique is able to segment the small/tiny vessels with the same level of accuracy as for the major/thick vessels.

The proposed method also has a higher  $SE$  compared to our previous method discussed in [6] and the other rival techniques. The maximum  $SE$  of 0.85 is obtained for the image '19\_test.tif' with a  $PPV$  of 0.762 from the DRIVE database. The minimum  $SE$  obtained on the DRIVE database is 0.7052 for the image '11\_test.tif' with a  $PPV$  of 0.7467. Our future work is to use this improved version of vessel segmentation algorithm in developing an automatic DR screening method.

## ACKNOWLEDGMENT

We would like to thank the authors of the DRIVE database for making their database free to download and use for the research purposes. We would also like to thank Education New Zealand for supporting this research financially, by providing the New Zealand International Doctoral Research Scholarship (NZIDRS).

## REFERENCES

- [1] H. Fu, Y. Xu, D. W. K. Wong, and J. Liu, "Retinal vessel segmentation via deep learning network and fully-connected conditional random fields," *IEEE 13th International Symposium on Biomedical Imaging (ISBI)*, pp. 698–701, 2016.
- [2] M. Melinsca, P. Prentasic, and S. Loncaric, "Retinal vessel segmentation using deep neural networks," *10th International Conference on Computer Vision Theory and Applications*, vol. 1, pp. 577–582, 2015.
- [3] D. Maji, A. Santara, S. Ghosh, D. Sheet, and P. Mitra, "Deep neural network and random forest hybrid architecture for learning to detect retinal vessels in fundus images," *37th Annual International Conference of the IEEE Engineering in Medicine and Biology Society (EMBC)*, pp. 3029–3032, 2015.
- [4] A. D. Hoover, V. Kouznetsova, and M. Goldbaum, "Locating blood vessels in retinal images by piecewise threshold probing of a matched filter response," *IEEE Trans. Med. Imag.*, vol. 19, no. 3, pp. 203–210, 2000.
- [5] J. Staal, M. D. Abramoff, M. Niemeijer, M. A. Viergever, and B. van Ginneken, "Ridge-based vessel segmentation in color images of the retina," *IEEE Transactions on Medical Imaging*, vol. 23, no. 4, pp. 501–509, 2004.
- [6] R. J. Chalakkal and W. Abdulla, "Automatic segmentation of retinal vasculature," *IEEE International Conference on Acoustics, Speech and Signal Processing (ICASSP)*, pp. 886–890, 2017.
- [7] R. Vega, G. Sanchez-Ante, L. Falcon-Morales, H. Sossa, and E. Guevara, "Retinal vessel extraction using lattice neural networks with dendritic processing," *Computers in biology and medicine*, vol. 58, pp. 20–30, 2015.
- [8] E. Ricci and R. Perfetti, "Retinal blood vessel segmentation using line operators and support vector classification," *IEEE Transactions on Medical Imaging*, vol. 26, no. 10, pp. 1357–1365, 2007.
- [9] M. M. Fraz, P. Remagnino, A. Hoppe, B. Uyyanonvara, A. R. Rudnicka, C. G. Owen, and S. A. Barman, "An ensemble classification-based approach applied to retinal blood vessel segmentation," *IEEE Transactions on Biomedical Engineering*, vol. 59, no. 9, pp. 2538–2548, 2012.
- [10] S. Roychowdhury, D. D. Koozekanani, and K. K. Parhi, "Blood vessel segmentation of fundus images by major vessel extraction and subimage classification," *IEEE Journal of Biomedical and Health Informatics*, vol. 19, no. 3, pp. 1118–1128, 2015.
- [11] Y. Q. Zhao, X. H. Wang, X. F. Wang, and F. Y. Shih, "Retinal vessels segmentation based on level set and region growing," *Pattern Recognition*, vol. 47, no. 7, pp. 2437–2446, 2014.
- [12] M. M. Fraz, S. A. Barman, P. Remagnino, A. Hoppe, A. Basit, B. Uyyanonvara, A. R. Rudnicka, and C. G. Owen, "An approach to localize the retinal blood vessels using bit planes and centerline detection," *Computer methods and programs in biomedicine*, vol. 108, no. 2, pp. 600–616, 2012.
- [13] X. Jiang and D. Mojon, "Adaptive local thresholding by verification-based multithreshold probing with application to vessel detection in retinal images," *IEEE Transactions on Pattern Analysis and Machine Intelligence*, vol. 25, no. 1, pp. 131–137, 2003.
- [14] A. M. Mendonca and A. Campilho, "Segmentation of retinal blood vessels by combining the detection of centerlines and morphological reconstruction," *IEEE Transactions on Medical Imaging*, vol. 25, no. 9, pp. 1200–1213, 2006.
- [15] B. Al-Diri, A. Hunter, and D. Steel, "An active contour model for segmenting and measuring retinal vessels," *IEEE Transactions on Medical Imaging*, vol. 28, no. 9, pp. 1488–1497, 2009.
- [16] A. R. Robertson, "Historical development of cie recommended color difference equations," *Color Research Application*, vol. 15, no. 3, pp. 167–170, 1990.
- [17] R. S. Berns and D. M. Reiman, "Color managing the third edition of billmeyer and saltzman's principles of color technology," *Color Research Application*, vol. 27, no. 5, pp. 360–373, 2002.
- [18] K. Zuiderveld, "Contrast limited adaptive histogram equalization," *Graphics Gems IV, Academic Press Professional, Inc.*, pp. 474–485, 1994.
- [19] P. Perona and J. Malik, "Scale- space and edge detection using anisotropic diffusion," *Pattern Analysis and Machine Intelligence, IEEE Transactions on*, vol. 12, no. 7, pp. 629–639, 1990.
- [20] F. W. Billmeyer, "Color science: Concepts and methods, quantitative data and formulae," *Color Research Application*, vol. 8, no. 4, pp. 262–263, 1983.
- [21] J. P. Serra, *Image analysis and mathematical morphology*. London ; New York: Academic Press, 1982.
- [22] M. Basu, "Gaussian-based edge-detection methods-a survey," *IEEE Transactions on Systems, Man, and Cybernetics, Part C: Applications and Reviews*, vol. 32, no. 3, pp. 252–260, 2002.
- [23] E. Cands, L. Demanet, D. Donoho, and L. Ying, "Fast discrete curvelet transforms," *Multiscale Modeling Simulation*, vol. 5, no. 3, pp. 861–899, 2006.
- [24] M. S. Miri and A. Mahloojifar, "Retinal image analysis using curvelet transform and multistructure elements morphology by reconstruction," *IEEE Transactions on Biomedical Engineering*, vol. 58, no. 5, pp. 1183–1192, 2011.
- [25] R. C. Johnson, S. J. Padmagireesan, A. Raheem, and A. V. Pillai, "Comparison of curvelet and contourlet transforms for retinal analysis," *Annual IEEE India Conference (INDICON)*, pp. 1214–1217, 2012.
- [26] E. A. E. Quinn and K. G. Krishnan, "Retinal blood vessel segmentation using curvelet transform and morphological reconstruction," *Emerging Trends in Computing, Communication and Nanotechnology (ICE-CCN), International Conference on*, pp. 570–575, 2013.
- [27] Z. Zhen-Bing, Jin-Sha, Yuan, Q. Gao, and Y.-H. Kong, "Wavelet image de-noising method based on noise standard deviation estimation," *International Conference on Wavelet Analysis and Pattern Recognition, 2007. ICWAPR '07.*, 2007.
- [28] J. Zhang and J. Hu, "Image segmentation based on 2d otsu method with histogram analysis," *International Conference on Computer Science and Software Engineering*, vol. 6, pp. 105–108, 2008.
- [29] A. Rosenfeld and John Pfaltz, "Sequential operations in digital picture processing," *Journal of the ACM (JACM)*, vol. 13, no. 4, pp. 471–494, 1966.